Simulation analysis of the processes in plasma spray applications

T. Zhu, M. Baeva, H. Testrich and R. Foest

Leibniz Institute for Plasma Science and Technology, Greifswald, Germany

Abstract: The behaviour of particles injected into the plume region of a thermal plasma jet is analysed by means of a model of particle tracing in pure Ar and mixtures Ar/H_2. This model accounts for heating and melting of the particles and allows one to obtain the particle trajectories, velocities, and temperatures. Statistical distributions of the particle size, angle and velocity of injection based on the real experimental conditions are taken into account. A model of the droplet impingement is employed to simulate the growth of the coating.

Keywords: Jet plume, particle tracing, droplet impingement, coating.

1. Introduction

Plasma spray torches are widely used in industrial applications concerning the deposition of protective and functional coatings. The quality and the properties of the produced coatings result from the processes on the entire chain: the operation conditions of the plasma torch, which are related to the characteristics of the electric arc and the generated plasma jet; the feeding of the powder material and its behaviour in the plasma jet; the deposition of the molten particles on the target. Previous studies have been focused on the characterization of the plasma spray torch [1,2] and the heating of the injected powder material into the jet plume [3]. In this work, the processes in the jet plume concerning the properties of the droplets that impinge onto the target are analysed and the formation of the coating is simulated.

2. Characteristics of the jet plume

The processes occurring in the plume region of the jet depend on the properties of the plasma. The latter are obtained in the framework of a three-dimensional model that solves the Navier-stokes equations for conservation of mass, momentum and energy with account for turbulent effects in a plasma in the state of local thermodynamic equilibrium. The model of the plasma spray torch [1] provides the boundary conditions at the torch exit. The model of the jet plume is described in more details in a previous work [3]. The distributions of the jet velocity and temperature in the central cut plane of the cylindrical computational domain are shown in Figure 1 for operations in pure Ar and in a gas mixture Ar/H_2 at atmospheric pressure and flow rates of respectively 40 NLPM and 40/14 NLPM for an arc current of 600 A. Notice that the jet axis is denoted as z and it starts at the exit of the plasma torch (z=0). The target is placed at the axial position z=120 mm and is perpendicular to the jet axis. The vertical direction is denoted as x. The powder material is fed by a carrier gas (Ar) with a flow rate of 3.4 NLPM. It has been approved that the injection of the powder material and the cold carrier gas does not affect the plasma properties.

The admixture of hydrogen results in a narrower plasma jet in the mixture than in pure argon. The isotherms in Fig. 1b) show a steeper decrease in the plasma temperature in the mixture for axial positions z ~ (10-30) mm. For axial positions z ~ (30-60) mm, the plasma temperature in argon remains well above that in the mixture. Towards the target, the plasma temperature of 1750 K in the mixture becomes by about 320 K higher than that in argon.

The jet velocity in the Ar/H_2 mixture is higher than that in pure argon over the whole distance (Fig. 1c,d). Notice that at small distances from the torch exit (z=0), the jet velocity in the mixture is by far larger than that in pure argon. This effect is explained by the decrease of the mass density in the mixture with hydrogen and the conservation of mass continuity [3].

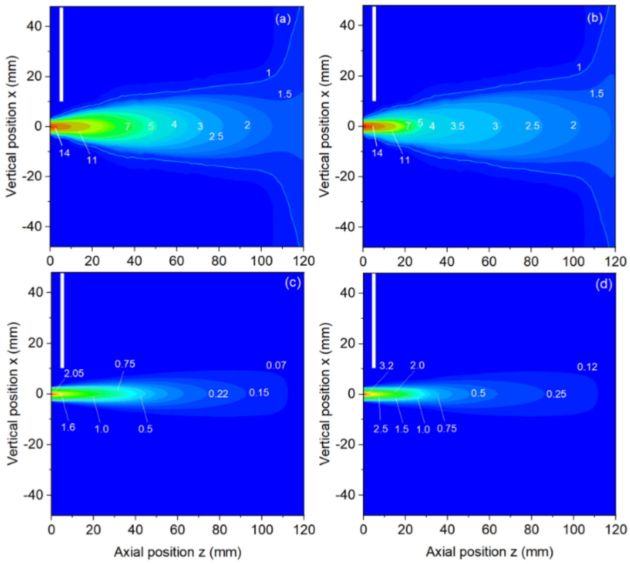

Fig. 1. Distribution of the temperature in 10^3 K (a,b) and the velocity magnitude in 10^3 m/s (c,d) of the plasma jet for operation in Ar (a,c) and Ar/H_2 (b,d).

In the recent work [3], we reported on the effect of fluctuating heating of the injected particles in the Ar/H_2 mixture. This effect results from particular dependence of the effective thermal conductivity (the sum of the thermal conductivity of the plasma gas (λ) and that caused by the turbulence (λ_T)) on the plasma temperature. The distributions of λ and $\lambda+\lambda_T$ at different axial positions in the jet plume are shown in Fig. 2a) and 2b). The effective thermal conductivity $\lambda+\lambda_T$ exceeds λ by one up to two orders of magnitude. Notice that the scale of $\lambda+\lambda_T$ is on the left hand side, while that of λ is on the right hand in Fig. 2. In the mixture Ar/H_2, the values of $\lambda+\lambda_T$ are not only significantly larger than those for pure argon, but they also exhibit a multi-peak course along the jet axis. Fig. 2b) shows the values of λ and $\lambda+\lambda_T$ along a line out, which is taken perpendicular to the torch axis at a distance z = 7 mm (this is approximately the position of the tube for the particle injection). In the perpendicular direction, the values of $\lambda+\lambda_T$ for the mixture show two off axis peaks.

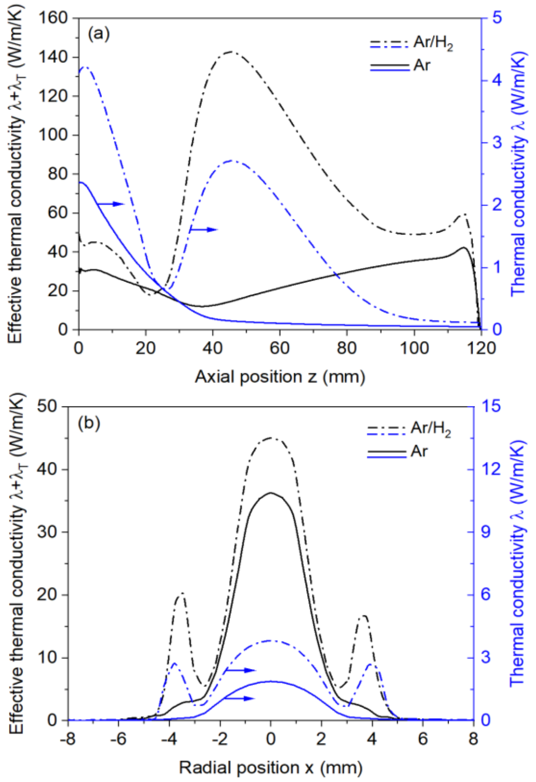

Fig. 2 Distribution of the effective thermal conductivity $\lambda+\lambda_T$ and the thermal conductivity λ along the jet axis (a) and the line out at z=7 mm (b).

3. Heating of the injected particles in the jet plume

The particles made of Al_2O_3 that are injected into the jet plume undergo heating and melting before they impinge onto the target. These processes are simulated by means of a model for particle tracing. The model is described in detail in the recent work [3]. Here, its main features are summarized for the sake of completeness. The particle tracing model solves the equation of motion of a particle accounting for forces acting on it. These are the drag, gravity, and the thermophoretic forces. Simultaneously, the particle heating is considered by solving a heat balance equation, which account for convective and radiative heat transfer. Particles with different size are randomly released on the exit plane of the feeding tube. The size distribution of the particles obeys a normal distribution with a mean value of 52.9 µm and a standard deviation of 20.5 µm. A random distribution is also applied to specify the initial velocity distribution of the particles, including the magnitude and angle. The effect of turbulent dispersion leading to a random change in the velocity magnitude and the direction of the particle motion is taken into account. This effect is more important for small particles. The particle temperature is assumed to be uniform. A statistically significant number of 3000 particles is considered. In the following, three selected particles (P658, P678, and P733) of size 20.0 µm, 37.0 µm, and 67.6 µm, respectively, are analysed with respect to the convective and radiative heat power sources determining their temperatures.

Fig. 3a) presents the convective heat power source Q_{conv} assigned to the selected particles along their trajectories starting with the injection until the impingement on the substrate. The notations are as follows: curves 1, 3, and 5 show the behaviour of respectively particles P658, P678,

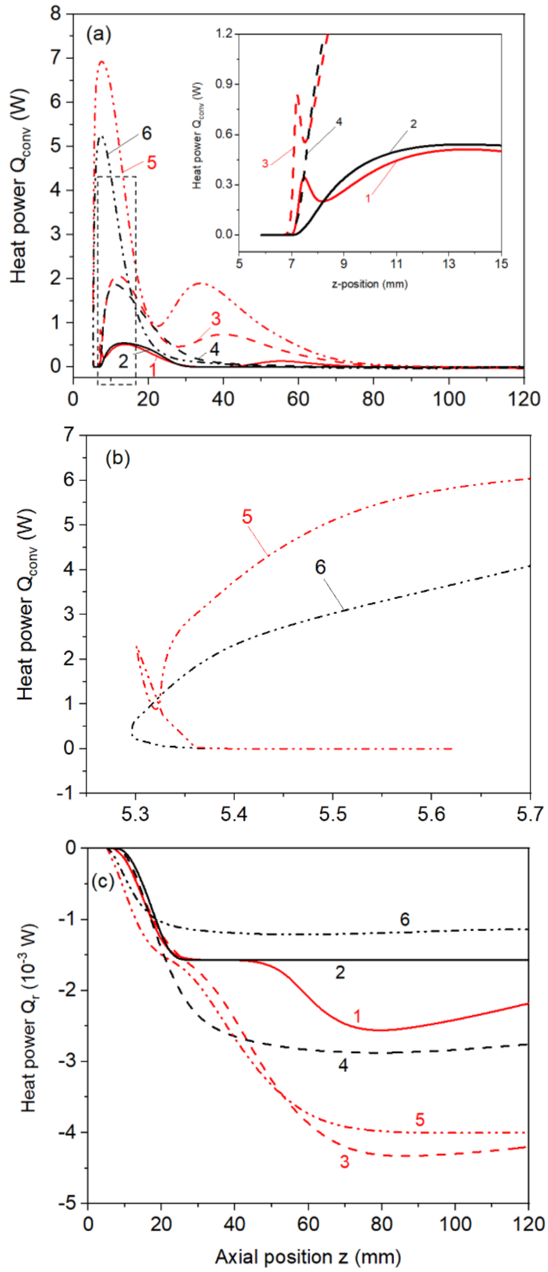

Fig. 3 Distribution of the convective Q_{conv} and the radiative heat power Q_{rad} for the selected particles in the jet plume. Notations: 1– P658 in Ar/H_2, 2– P658 in Ar; 3 – P678 in Ar/H_2, 4 – P678 in Ar, 5 – P733 in Ar/H_2, 6 – P733 in Ar.

and P733 in the mixture Ar/H_2, while curves 2, 4, and 6 correspond to the behaviour in pure argon of particles P658, P678, and P733, respectively. Notice that a particle can cross the same axial position more than once along its trajectory. Along the particle trajectories, Q_{conv} for all particles shows in the mixture Ar/H_2 several peak values. This indicates that particles in Ar/H_2 jet experience a spatially fluctuating heating. In the region close to the injection tube (z ~7 mm), the fluctuating heating phenomena is also present (see the enlarged part in Fig. 3a). In pure Ar, the injected particles experience just one single heating peak during their flight. This corresponds to the results presented in Fig. 2. For the largest particle P733, the fluctuating heating effect is not well seen in the enlarged part in Fig. 3a) due to the upstream shift of the second heating peak. This case is shown separately in Fig. 3b). Apparently, the particle P733 was initially injected in direction opposite to the z and was then carried by the jet in the positive z direction. Interesting, the particle P733 experiences the fluctuating heating while moving in the -z direction. Fig. 3c) shows the radiative heat power source Q_{rad} for the three particles. In general, it can be seen that Q_{rad} is stronger for larger particles because of the larger surface area.

Figures 4a,b) show the development of respectively the particle temperature and velocity during the motion in the plasma jet. The temperature of small particles increases rapidly and reaches the melting point T_m at *z* -positions between 20 mm and 30 mm in both Ar/H_2 (curve 1) and pure Ar (curve 2). The temperature of larger particles remains below the T_m-value in both gases (curves 3, 4 and 5, 6) even though the heat source of large particles can be larger. These can be explained by the different factor of increase of the particle surface and mass with the increase of the particle diameter.

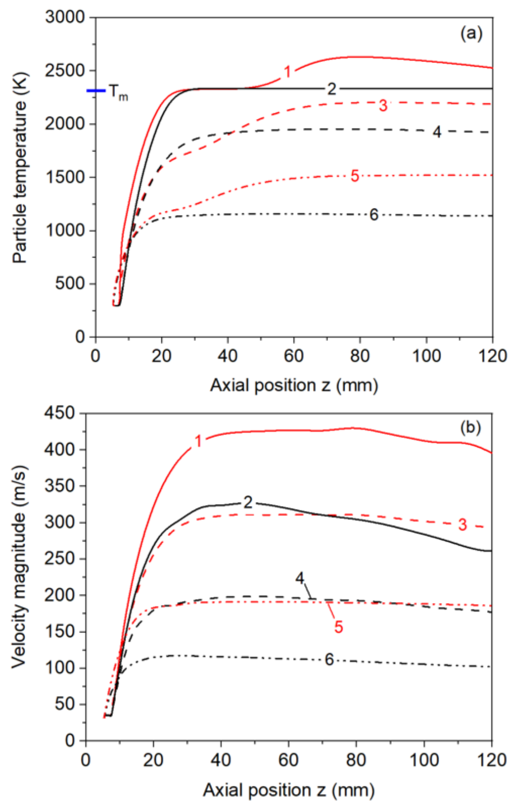

Fig. 4 Temperature and velocity of the particles. The notations of the curves are the same as in Fig. 3.

4. Impingement of a particle onto the substrate and coating building

Heated and molten particles (droplets) reach the substrate and a coating is built. During the time of deposition, a droplet undergoes changes in phase and in shape, heat exchange with the ambient gas and the substrate occurs before solidification. A model of a single droplet impinging on the substrate has been established in order to capture the evolution details of the process. To trace the free interface between liquid phase and ambient gas, level set method is applied. This method allows us to compute evolved curved surfaces on a Cartesian grid without the need to parameterize the curved surfaces. The model further solved the fluid flow, the conservation of mass, momentum and energy for the droplet and the ambient gas. The particle tracing model provides the input parameters (temperatures and velocities of the droplets).

The impengement of an Al_2O_3 droplet with a radius of 25 µm is shown in Fig. 5. It is located at a distance of 10 µm above the substrate with an initial downward velocity of 200 m/s and a temperature of 2400 K. A contact angel of

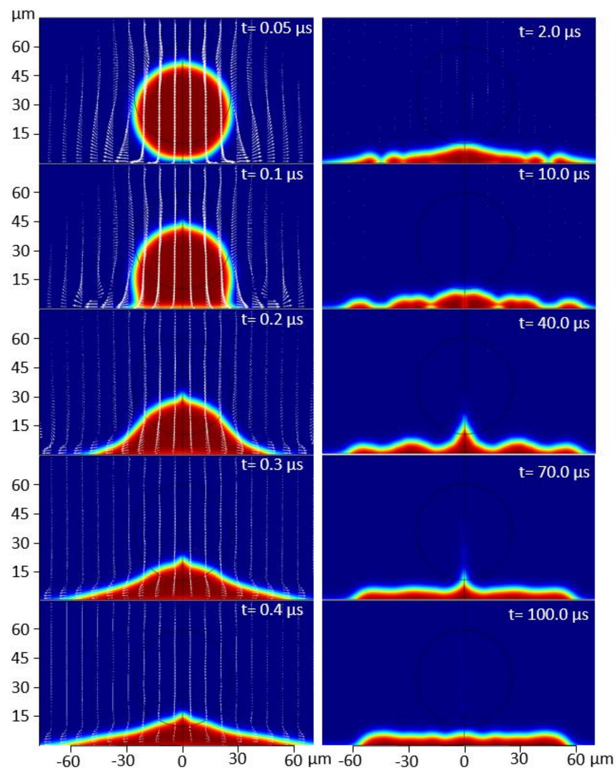

Fig. 5 Distribution of volume fraction of Al_2O_3 droplet during impingement process onto substrate.

94° is specified. A series of snapshots shows the shape change of the droplet. The arrows represent the velocity of the droplet and the ambient gas. Within 0.1 µs, the droplet starts to expand radially once it is in contact with the substrate. The radial spreading is limited by the surface tension. The radial extent of the surface coverage reaches a value of about 60 µm and the height is about 4.7 µm.
The building of the coating due to the subsequent impingement of droplet after droplet is not further followed since this would require a change in the topology of the problem. Instead, the growth of the coating is simulated by means of a modified boundary condition in the framework of the particle tracing model, which makes use of an accumulator variable. The accumulator variable is defined in every element on the surface and is raised when a droplet collides with the surfaces. The average increment for the variable of 4.7 µm is derived from single droplet impingement model with values of the temperature and velocity under spraying conditions. The value of the accumulator variable corresponding to the end of the computation provides the coating thickness. The distribution of the coating thickness on the substrate plane for different working gases is shown in Fig. 6. Notice that the position characterized by coordinates (x,y) =(0,0) corresponds to the cross point of the jet axis. The results show that both in Ar (Fig. 6a) and in Ar/H_2 (Fig. 6b), the most of the particles are accumulated at positions x<0, i.e. in the area below the cross point with the jet axis.
In Ar/H_2, the droplets are less scattered and therefore, larger thickness values are obtained.

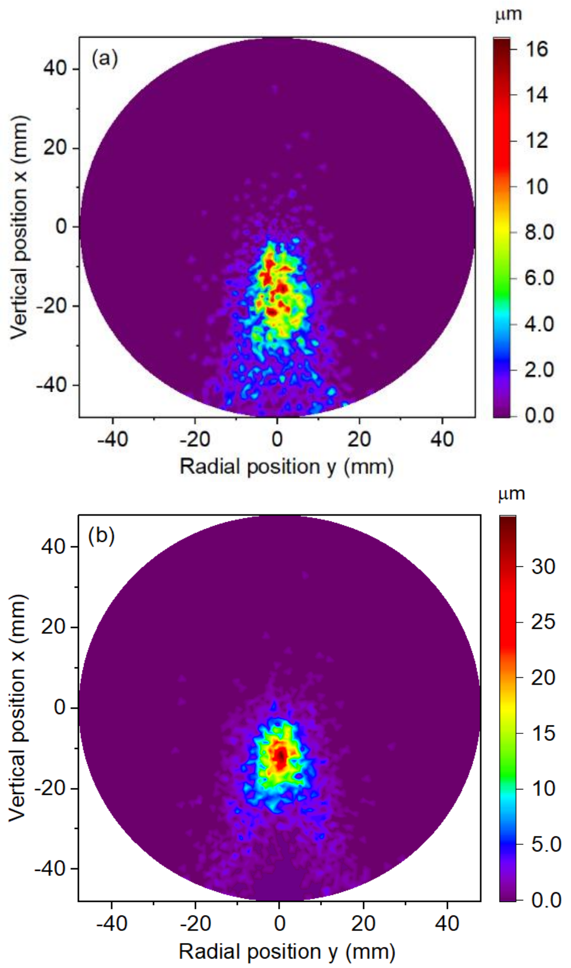

Fig. 6 The thickness of the built on the target surface during operation in (a) Ar, (b) Ar /H_2.

5. Conclusions

In this work, processes occurring in the plume region of a plasma spray torch, where powder material of Al_2O_3 is injected have been analysed. The plasma spray torch is operated at an arc current of 600 A in Ar and Ar/H_2 with flow rates of respectively 40 NLPM and 40/14 NLPM. The results can be summarized as follows.
In the mixture Ar/H_2, the plasma jet is narrower and is characterized by a rapid decrease of the temperature for distances of (10-30) mm from the torch exit. In front of the substrate, which is placed in a distance of 120 mm away from the torch exit, the temperature the mixture is about 1750 K and about 320 K higher than that in argon.
The behavior of the Al_2O_3 particles injected into the jet plume depends strongly on their size. Small particles (diameter of about 20 µm) are molten in both Ar and in Ar/H_2 but higher droplet temperatures are reached in Ar/H_2. The particles undergo a spatially fluctuating heating in Ar/H_2, which results from the temperature dependence of the effective thermal conductivity.
The accumulation of droplets on the substrate is less scattered during operation in Ar/H_2 and thicker coatings can be obtain in the mixture than in pure Ar.
The predictions of the simulations contribute to the adjustments of the torch handling during the experiment under real spraying conditions.

6. Acknowledgment

This work was funded by the European Union and the Federal State of Germany Mecklenburg-Western Pomerania (Project number TBI-V-1-321-VBW-112). The authors thank Y. Cressault from University of Toulouse (France) for providing the radiation data for the Ar/H_2 mixture.

7. References

[1] M. Baeva, T. Zhu, T. Kewitz, H. Testrich, R. Foest, Journal of Thermal Spray Technology, **30**, 1737 (2021).
[2] M. Baeva, M. S. Benilov, T. Zhu, H. Testrich, T. Kewitz, R. Foest, Journal of Physics D: Applied Physics, **55**, 365202 (2022).
[3] T. Zhu, M. Baeva, H. Testrich, T. Kewitz, R. Foest, Plasma Chemistry and Plasma Processing, **43**, 1 (2023).